Surface Diffusion of Poly(ethylene glycol)

Svetlana A. Sukhishvili,[†,§] Yan Chen[⊥,‡,] Joachim D. Müller[⊥,‡,] Enrico Gratton,[‡] Kenneth S. Schweizer,[†] and Steve Granick*[,†]

Department of Materials Science and Engineering, University of Illinois, Urbana, Illinois 61801, and Laboratory for Fluorescence Dynamics, Department of Physics, University of Illinois, Urbana, Illinois 61801

Received July 30, 2001; Revised Manuscript Received December 17, 2001

ABSTRACT: We report direct measurement of the center-of-mass diffusion coefficient, D, of uncharged flexible linear chains adsorbed at the solid−liquid interface at dilute surface coverage. We find $D \sim N^{-3/2}$ (N is degree of polymerization) when N was varied by more than an order of magnitude ($N = 48$, 113, 244, 456, and 693) and the scatter of the data was low. The experimental system was poly(ethylene glycol), PEG, adsorbed from dilute aqueous solution onto a self-assembled hydrophobic monolayer, condensed octadecyltriethoxysilane. The method of measurement was fluorescence correlation spectroscopy of a rhodamine green derivative dye that was end-attached to one sole end of the adsorbed PEG chains. The observed scaling implies the diffusion time $\tau \sim N^3$ if $R_g \sim N^{3/4}$ as expected for a chain in good solvent in two dimensions (R_g is the radius of gyration), but a variety of other theoretical approaches to describe the dynamical scaling are also plausible. The multiplicity of plausible dynamical transport scenarios is compounded by the fact that polymer diffusion is sensitive to chain conformation on the surface which is not directly observable. Various theoretical scenarios are explored, and the need for new experiments, theory, and computer simulation studies to allow definitive interpretation of this observation of simple and clean fractional power law scaling is emphasized.

Introduction

That dynamics of polymer chains at and near solid interfaces differs profoundly from that in the bulk is intuitively expected. Nonetheless, concerning even the simplest imaginable case, polymer without attraction to the surface, one concludes that the situation is complex. Intramolecular conformations, and even the local density of polymers in solution and in the undiluted melt state, may be anisotropic in the directions parallel and normal to a surface and furthermore may vary with distance normal to that surface. Structure and dynamics may be further influenced by attractive interaction of molecules with the surface and by topographical and chemical heterogeneity of the surface itself. So many variables come into play that one is at an early stage in the attempt to formulate unifying general principles.

For a time it seemed self-evident that segmental mobility in the liquid state must be speeded up near a nonadsorbing surface. There is ample simulation evidence in favor of such an idea[1] due to the fact that random coils orient preferentially parallel to a solid boundary for steric reasons.[2] Attractive forces between polymer segments and the surface, and surface corrugation, might of course slow everything down. This would be so not just because of altered chain conformations, which would present additional points of contact with the surface compared with the case of a random coil, but also because motion might then be rate-limited by Arrhenius adsorption−desorption events rather than by intersegmental monomeric friction. There is copious evidence from experiment[3,4] and many computer simulations of the qualitative effect.

However, even this conclusion turns out to be controversial. It seems that the glass transition temperature may be depressed in the same systems where near-surface diffusion is observed to be retarded.[3,4] Controversies concerning the glass transition in thin polymer films show the impossibility, at the current state of understanding, of generalizing about even the attractive case when comparing different chemical systems.[5]

The diffusion of molecules within monolayers at a surface is potentially a simpler case with which to begin. The related question of protein diffusion within lipid membranes at submonolayer coverage has been studied exhaustively.[6−8] The question asked in this field was how center-of-mass diffusion scales with concentration in the monolayer. Reasonable agreement was found with theories that model the molecule as a compact-shaped solid object. These models also seem to describe the scaling of the diffusion coefficient with surface concentration when flexible polymers are spread at submonolayer coverage at the water−air interface.[9]

Consider now surface diffusion of flexible chains of various degree of polymerization (N). Do the individual segments diffuse locally as independent actors? If not, how should their correlated motions be modeled? The computer simulations of Carmesin and Kremer for a literally 2-dimensional solution found no evidence of strong correlations when considering the case of dilute chains in the absence of hydrodynamic interactions.[10] In other words, the center-of-mass diffusion coefficient, D, scaled as $D \sim N^{-1}$ (Rouse behavior). A surface that contains impenetrable obstacles which require the chain to diffuse around them does strengthen the dependence on N,[11,12] but different simulation studies seem not to agree on the consequences of such obstacles on the N scaling of D. We return to this in the Discussion section.

[†] Department of Materials Science and Engineering.
[‡] Department of Physics.
[§] Present address: Department of Chemistry and Chemical Biology, Stevens Institute of Technology, Castle Point on Hudson, Hoboken, NJ 07030.
[⊥] Present address: Department of Physics, University of Minnesota, Minneapolis, MN 55455.

10.1021/ma0113529 CCC: $22.00
Published on Web 02/01/2002

The pioneering experiment of Maier and Rädler,[13] concerning diffusion of DNA, an anionic polymer, adsorbed to dilute submonolayer coverage onto a cationic fluid lipid membrane, also found $D \sim N^{-1}$, the prediction of the Rouse model without hydrodynamic interaction. This experiment considered stiff DNA chains, long enough to visualize in an optical microscope, and which have statistical segments such that the molecular conformations obeyed random walk statistics with excluded volume. The Coulombic interactions responsible for binding the chain to the surface are inherently long-range. It is worth asking whether a system dominated by short-range interactions, as expected for nonpolar polymers, would behave similarly. Second, because the lipid membrane used as a surface in those experiments was in the fluid phase, it is conceivable that reorganization of molecules within the fluid membrane might compete with motions of adsorbed DNA molecules as the rate-limiting step that controlled the center-of-mass diffusion. If reorganization of the fluid membrane were indeed the rate-determining step, this could be an alternative explanation for the observed $D \sim N^{-1}$. Moreover, surface fluidity would serve to efficiently dissipate polymer−solvent hydrodynamic forces.

For these reasons we have turned to a solid surface (rather than fluid membrane) and to an uncharged, synthetic polymer. The small size of the synthetic polymer precluded direct optical imaging as in the study of DNA.[13] We adopted instead fluorescence correlation spectroscopy, FCS, a technique developed in the biophysics community that is capable of measuring dynamics even of single molecules.[14,15] A very brief account of this work was recently presented.[16]

Experimental Section

Materials. Poly(ethylene glycol) (PEG) was selected for study because monodisperse amino-terminated PEG with a wide range of molecular weight are available commercially. A fluorescent label can be attached using methods that are well-established in protein chemistry.[17] The parent PEG samples with weight-average molecular weights 2200, 5000, 10 800, 20 100, and 30 500 g mol^{-1} (degree of polymerization N = 48, 113, 244, 456, and 693, respectively) and ratio of weight-average to number-average molecular weight M_w/M_n = 1.01−1.03 were purchased from Shearwater Polymers, Inc. The molecules contained the methoxy group at one terminus and amino group at the other one (PEG-NH_2). In some surface experiments, we used a sample of the unlabeled polymer, PEG monomethyl ester, as a "blank" and mixed it with labeled PEGs in various proportions to reduce the density of fluorophores in the adsorbed layer. This sample was terminated by a hydroxyl instead of an amino group (PEG-OH) and had a molecular weight 5000 and M_w/M_n = 1.01.

Two fluorescence labels were used. One was fluorescein 5-isothiocyanate (FITC) purchased from Sigma, and another one was Alexa-488 purchased from Molecular Probes as a kit for protein labeling.

The H_2O was double-distilled and further purified by passage through Milli-Q (Millipore) deionizing and filtration columns.

Protocol to Label PEG-NH_2 with FITC. For studies of diffusion in bulk solution, the PEG samples were labeled by fluorescein 5-isothiocyanate (FITC), which is less costly than Alexa-488. The procedure was based on the well-known protocol for labeling of proteins, which involves chemical reaction between the isothiocyanate group of the label and amino group of the protein.[17,18] In this work the labeling was done in organic solvent.

Specifically, 2−4 wt % dichloromethane solution containing PEG-NH_2 was mixed with 0.4−1 wt % ethanol solution of FITC (5−10-fold molar excess of the label to amino groups in the polymer terminus). After 1 h, the polymers were precipitated into cold diethyl ether. Because of the partial solubility of FTIC in diethyl ether, the polymers were cleaned from the excess of unbound label at this step. The procedure was repeated four times until the ratio of FTIC to PEG molecules in the precipitating product was constant.

Note that this procedure was changed for the modification of the PEG-NH_2 of lowest molecular weight, 2000, because it appeared to dissolve in ethyl ether. This polymer was precipitated into hexane, and tetrahydrofuran was used as a solvent for the labeling. The precipitates were separated from the diethyl ether or hexane, filtered, and dried in a vacuum. The labeled polymers were yellow-orange in color.

To estimate the degree of labeling of the polymers, the molar extinction coefficient of unbound FTIC molecules at 493 nm was determined; 0.001 M borate buffer was used as a solvent. The resulting value of 84 000 AU L mol^{-1} cm^{-1} agrees well with the value 76 800 AU L mol^{-1} cm^{-1} reported earlier by others (AU = absorbance units).[18]

The amount of PEG in the labeled fractions was determined by transmission IR spectroscopy of the polymer solutions in 0.001 M borate buffer. The experiment was done in a liquid cell with CaF_2 windows and path length of 25 μm. For calibration, the height of the peak located at 1096 cm^{-1}, which is associated with C−O −C stretching vibration, was determined for PEG aqueous solutions of known concentration. The degree of labeling was determined as 98%, 70%, 86%, and 90% for the PEGs with molecular weights 2200, 5000, 10 800, and 20 100, respectively.

Protocol to Label PEG-NH_2 with Alexa-488. The fluorescent end-label for the studies of surface diffusion was chosen to be Alexa-488 (Molecular Probes, Inc.), a derivatized rhodamine green molecule with exceptionally bright fluorescence and stability against photodegradation. Our initial attempts to use the FITC label for surface studies failed owing to photodegration at the surface, though not in solution.

Alexa-488 reactive dye has a succinimidyl moiety and can be attached to amino groups of different molecules. The labeling reaction was conducted in a nonaqueous medium. In a typical labeling protocol, the label (∼0.3 mg) was dissolved in a 4:3:3 mixture of ethanol, dimethyl sulfoxide, and methylene chloride (total volume was 100 μL, ∼7 mM concentration of the label). Then ∼20 μL of label solution was quickly added to 10 μL of ∼2 mM solution of PEG-NH_2 in an ethanol/methylene chloride 3:1 mixture. The molar excess of labels to the polymer molecules in the reaction mixture was 6.5. After 1 h, the reaction mixture was diluted by ∼100 μL of aqueous 0.01 M phosphate buffer (pH = 8.4) to dissolve occasionally precipitated polymer; this solution was kept for 1 week and was diluted by 0.01 phosphate buffer (pH = 8.4) when necessary to get the required low concentrations of the labeled PEG molecules.

Because of the much higher price of the Alexa-488 fluorescent label compared to that of fluorescein, purification of the product by precipitation appeared troublesome, and a different procedure was used to separate the labeled PEG molecules from the unbound labels. In brief, we took advantage of the fact that the Alexa-488 label did not adsorb, but PEG molecules adsorbed strongly onto the OTE-modified surface. This allowed us to separate the unbound label from the labeled PEG molecules by simple copious exchange of the solution to the pure buffer after adsorption of the labeled polymer was complete.

To estimate the degree of labeling, we used a combination of ATR-FTIR and FCS techniques. In brief, the number of molecules per surface area for the saturated adsorbed layer was estimated from the FCS experiment, and IR measurements of the amount of PEG adsorbed (see below). These estimates showed that ∼70−90% of the PEG-NH_2 reacted with the Alexa-488 fluorescence label.

Chemical Modification of the Solid Surface. Since PEG does not adsorb from aqueous solution to hydrophilic fused silica at high pH,[19] the fused silica required for our optical experiment was derivatized by a monolayer of condensed octadecyltriethoxysilane (OTE) to render it hydrophobic. Prior

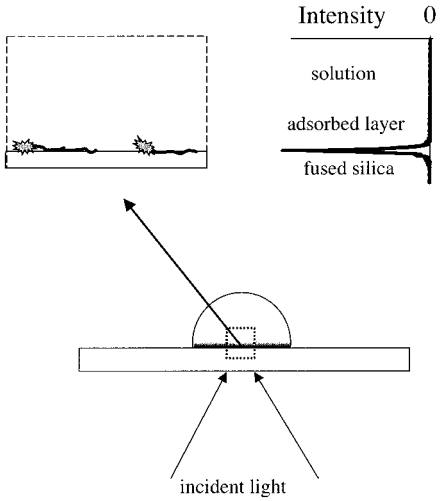

Figure 1. Schematic diagram of the strategy to measure two-dimensional polymer diffusion at the solid−liquid interface using fluorescence correlation spectroscopy (FCS) with an optical microscope. A droplet of solution, placed on a hydrophobized quartz coverslip within a sealed chamber, was illuminated at 780 nm by a focused laser beam (bottom sketch). This excited the fluorescence of labeled poly(ethylene glycol) (PEG) chains (top left sketch). When these chains were allowed to adsorb and then the surrounding solution was replaced with pure buffer, we detected fluorescence only when the laser beam was focused at the solid−liquid interface (the top right panel shows actual data), thus demonstrating that the PEG chains were irreversibly adsorbed to the interface. In separate experiments, when the optics were focused separate from the surface, diffusion of labeled PEG in the bulk solution was measured.

to self-assembly, fused silica slides were cleaned by UV-ozone treatment for 30 min and kept in a concentrated sulfuric acid−Nochromix solution. Slides were then copiously rinsed with water, dried with nitrogen, and treated in a UV-ozone plasma cleaner (Harrick Sci. Corp.) for 5 min. After that, they were rendered hydrophobic by allowing hydrolyzed OTE to self-assemble from a dilute hydrocarbon solution. The technique for monolayer self-assembly was described previously,[20] except that the oven-baking step was omitted. The advancing contact angle of water was approximately 95°.

For the infrared measurements, a silicon crystal was used as a substrate. The procedure to modify the crystal with a monolayer of self-assembled OTE was the same, except that before UV-ozone treatment the crystal was dipped momentarily in 5% HF solution to remove the surface oxide layer before growing it back by the controlled UV-ozone treatment.

Sample Cell for FCS. The sample cell for a typical FCS experiment in this study is shown schematically in Figure 1. It consisted of a thick glass slide, ∼12 mm thick, with ∼15 mm hole in the center. A 25 mm × 25 mm coverslip of ∼17 μm thickness, which was made from fused silica and coated for the experiment with an OTE monolayer, was attached to one side of it by using a hot wax. This sealing, as well as application of the low-viscosity oil for an oil immersion microscope objective, was found to reduce mechanical drift of the sample cell. A small amount (∼100 μL) of aqueous buffered polymer solution was then deposited on the hydrophobized quartz slide. It formed a drop with a contact angle of about 95°. To prevent solvent evaporation, the upper opening was covered with a clean glass cover slide. A small drop of water was put between the top cover slide and the sample cell to improve adhesion.

FCS Measurements. The method of measurement was two-photon fluorescence correlation spectroscopy (FCS) based on analyzing fluctuations of fluorescence as fluorophores diffuse in to and out of the small volume at the focus of incident light where intensity is high enough to excite fluorescence. FCS measures the mutual diffusion coefficient (D_M) of fluorescing species.[14,15] In dilute systems, such as the present experiment, $D_M \approx D_{CM}$ (D_{CM} is the center-of-mass diffusion coefficient).[21]

The instrumental setup for two-photon fluorescence correlation spectroscopy used in this work was similar to the one described earlier by Berland et al.[15] One of the major components in this setup is a mode-locked Ti−sapphire laser, with pulse width ∼100 fs and repetition rate of ∼80 MHz, which provides an efficient two-photon excitation light source. The wavelength of the laser was adjusted to 780 nm. The excitation light was then sent to a Zeiss Axiovert 135 TV microscope (Thornwood, NY). All the experiments were performed with 63× Plan Apochromat objective (numerical aperture 1.4), which has favorable aberration correction and a high transmission in the visible wavelength region. The high photon flux required for two-photon excitation only occurred at the microscope focus. The fluorescence, generated by the two-photon excitation of the sample, was then detected by an avalanche photodiode (EG&G, Canada). Finally, the photon counts were saved on a computer. The laser power at the sample was routinely low, as low as 140 μW, to avoid heating and photodegradation.

Data Analysis. The autocorrelation function of fluorescence fluctuations, $G(\tau)$, was calculated from photon counts measured as a function of elapsed time. For two-dimensional diffusion when the sample is illuminated by a Gaussian laser beam, $G(\tau)$ has the following functional form for a single species:

$$G(\tau) = G(0)(1 + 8D\tau/w_0^2)^{-1} \quad (1)$$

where w_0 represents the Gaussian beam waist, ∼0.32 μm for our experimental setup.

In this analysis, we suppose the operative transport process to be surface diffusion. In addition to surface diffusion there could be other processes, such as rotation of the dye, and adsorption and desorption of polymers to and from the surface. But rotation occurs on time scales (nanoseconds) too rapid to detect. FCS is not sensitive to kinetic processes that occur on time scales slower than the diffusion time through the laser spot. Thus, the FCS data have not ruled out absorption and desorption processes that occur on time scales larger than a few seconds. FCS would not detect these, because the probability of such an event is essentially nil during the time it takes for a polymer to diffuse through the laser spot. Adsorption and desorption taking place on faster time scales might give rise to an additional kinetic process in the autocorrelation function. However, on the time scales probed by the autocorrelation function, we did not see the presence of another kinetic process. Having ruled out this alternative, we are left with surface diffusion. The surface diffusion model fits the autocorrelation data within experimental error.

We also focused the laser beam above the surface. If there were binding kinetics to the surface, we should have observed an autocorrelation function from the desorbed polymer diffusing through the excitation volume. We have detected no fluorescence signal above the surface. This result is in agreement with polymer exchange experiments (described below), where we observed irreversible adsorption of these polymers.

The experimentally measured autocorrelation functions were directly fitted to eq 1 using programs written for PV-WAVE 6.10 (Visual Numerics, Inc.) and LFD Globals Unlimited software (Champaign, IL). Analysis of errors showed that the data at the shortest and largest times had larger scatter; this fact was taken into account in the fitting procedure.

Calibration of the Excitation Volume. FCS experiments measure directly the residence time of a molecule within the excitation volume. The diffusion coefficient of the sample of interest can be calculated if the excitation volume is calibrated. The excitation volume can be affected by optical alignment and should be calibrated for a particular experimental setup. We calibrated the excitation volume using fluorescein, a common dye with a diffusion coefficient of $D = 300$ μm^2/s, which was dissolved in 50 nM tris buffer at pH = 10. Beam waist diameter was found to be 0.32 μm. The excitation volume was elongated, with a longest dimension of ∼1.5 μm along the optical axis.[22] The use of fluorescent dyes in bulk solution to

calibrate the beam waists of the excitation volume is a standard procedure.

ATR-FTIR Measurements. Infrared spectra were collected using a Biorad FTS-60 Fourier transform infrared spectrometer (FTIR) equipped with a broad-band mercury cadmium telluride detector. The attenuated total reflection (ATR) optics and the thermostated home-built adsorption cell placed in a nitrogen-purged compartment external to the FTIR spectrometer were described previously.[23]

The beam was reflected 11 times as it traveled the length of the crystal. The crystal was a rectangular trapezoid of dimensions 50 mm × 20 mm × 2 mm (Harrick Scientific) whose beam entrance and exit surfaces were cut at 45°. The procedures to clean the silicon surface and cell elements and to prepare a reproducible oxide surface are a generalization of methods developed previously for adsorption studies of nonpolar polymers.[24] These methods were shown to reproducibly create an oxidized surface (primarily SiO_2 and SiOH) while minimizing the amount of organic contamination from the ambient laboratory.

The experiment began after the following protocols. First the cell was filled with buffered H_2O and equilibrated for an hour before a background spectrum was collected. Polymer solution was not added until 0.5−1 h after the cell had been filled with water or salt solution; this improved the baseline stability. Interferograms were collected with 4 cm^{-1} resolution. The usual number of scans was 512.

Determination of the Amount Adsorbed. Infrared spectroscopy in attenuated total reflection (FTIR-ATR) provided the absolute calibration of the relative amounts measured from fluorescence intensity. The infrared absorption peaks in the region of 2990 cm^{-1} were integrated for purposes of tracking the adsorbed mass. The data were analyzed using curve fitting of the absorption peaks.

The calibration procedure consisted of measuring the infrared absorbances of molecules in a solution that was exposed to a nonadsorbing surface.[23,24] In this study, the oxidized Si crystal was nonadsorbing since PEG did not adsorb from aqueous solutions at high pH (a 0.01 M phosphate buffer at pH 8.4 was used). The calibrated contribution of PEG-OH in solution gave an effective extinction coefficient of 0.023 AU per mg mL^{-1}. From this number and the known penetration depth (∼0.26 μm for the silicon crystal that we used and wavenumber ∼ 2990 cm^{-1}), the calibration constant to calculate the adsorbed amount was obtained. For the sum of CH_s and CH_{as} bands, this value was 0.182 AU m^2 mg^{-1}.

Results

Adsorption Isotherms. The amount of PEG-OH adsorbed at saturated surface coverage was determined in the ATR-FTIR experiment using a Si crystal coated with a self-assembled OTE monolayer. The procedure consisted in allowing the polymer to adsorb from 0.1 mg/mL solution in 0.01 M aqueous phosphate buffer with pH 8.4. The measured infrared absorbances stabilized after the short time span of 2 min. The procedure used to calibrate the amount adsorbed from the infrared signal is described in the Experimental Section.

In a control experiment we showed that polymer chains were irreversibly bound to the surface: no desorption was detected when polymer solution was copiously exchanged to a pure buffer. This is the behavior expected for a polymer attached to the surface in a flattened "pancake" conformation characterized by a very large activation energy for all segments of the adsorbed chain to leave the surface simultaneously. It is consistent with the data reported by other groups.[25]

The saturated amount adsorbed was 0.9 mg/m^2 for the PEG-OH with M = 5000 g mol^{-1}. This amounts to twice the single monolayer coverage when PEG is spread as a close-packed monolayer at the air−water interface,[26] which is consistent with the expected loop−train−tail conformation when the surface coverage is saturated rather than dilute.

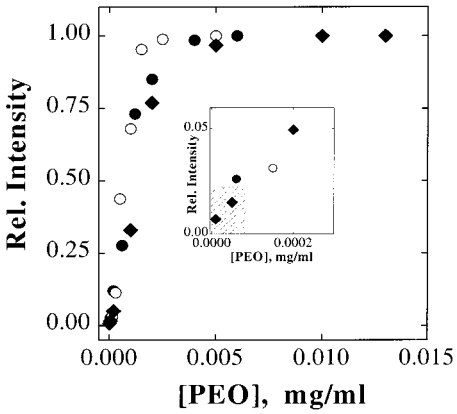

Figure 2. Relative intensity of fluorescence from the adsorbed layer is plotted as a function of the concentration of labeled PEG in solution for PEG samples with different degree of polymerization: N = 48 (filled diamonds), N = 113 (open circles), and N = 456 (filled circles). The fluorescent label was fluorescein isothiocyanate for PEG with N = 48 and was Alexa-488 for PEG with N = 113 and N = 456. Inset shows the same graph but enlarged in the region of low surface coverage. Shaded area refers to the conditions at which the diffusion experiment were done. The ionic concentration of the phosphate buffer was 0.01 M, and the pH was 8.4.

Next, the adsorption isotherms (amount adsorbed as a function of concentration in solution) were determined from the fluorescent intensity of adsorbed layers when the laser beam was focused at the interface so that intensity from the surface fluorescent species would assume maximum value. To avoid the self-quenching of the fluorescent labels when their concentration in the adsorbed layer were dense, we worked with 9:1 mixtures of unlabeled and labeled PEG polymers. In these experiments, PEG was first allowed to adsorb from a solution of very low concentration, ∼3−10 nM. Fluorescence intensity from the adsorbed layer stabilized after a waiting period of 40 min. Polymer solution was then copiously exchanged to a pure buffer. After the exchange, fluorescence intensity measured from the adsorbed polymer did not change. This confirms irreversibility of polymer adsorption. Polymer solution of higher concentration was then introduced by placing a drop on the surface, and the whole procedure was repeated until intensity from the surface was saturated. The adsorption isotherm is shown in Figure 2. One sees that the isotherms were of high affinity and saturated when bulk concentration of PEG was low, ∼0.002 mg/mL.

The segmental sticking energy has been estimated from the adsorption isotherm data at low PEG concentration for the N = 48 sample (inset of Figure 2) as described in the Discussion section. The analysis is consistent with the pancake interpretation. However, more experiments are required due to possible complications discussed below.

FCS Measurements of Diffusion. Diffusion experiments were restricted to cases when the surface coverage, gauged from the fluorescence intensity, was far less than the saturated monolayer coverage described above. Control experiments showed that the fluorescent labels by themselves did not adsorb, thus confirming that the labels had no specific affinity for the surface.

Figure 3 displays the normalized autocorrelation functions, $g(\tau)$, of PEG with N = 48 and N = 693 plotted

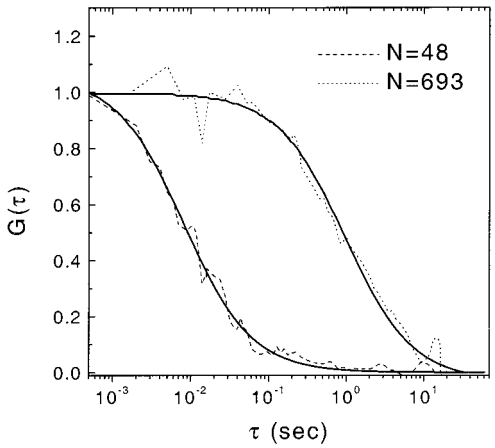

Figure 3. Fluorescence autocorrelation functions, $g(\tau)$, normalized to unity, are plotted against logarithmic delay time, τ ($N = 48$ and $N = 693$ at surface coverage 0.01 mg m^{-2}). The data were fitted to the expression $G(\tau) = G(0)(1 + 8D\tau/w_0^2)^{-1}$, which is valid for a two-dimensional Gaussian beam profile defined by the focused laser beam assuming a single diffusing species. Here the fluctuation amplitude $G(0)$ is inversely proportional to the number of molecules in the excitation volume, and w_0 is the Gaussian beam waist. The fit of this expression to the data demonstrates a single diffusion time.

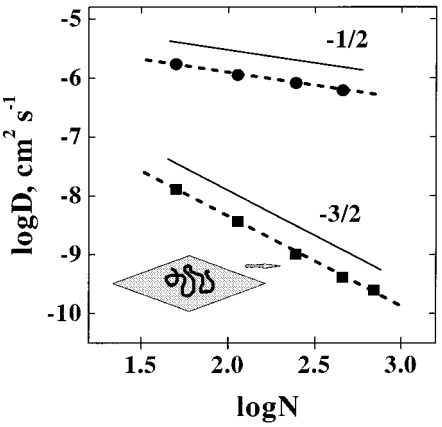

Figure 4. Center-of-mass diffusion coefficients, D, are plotted on log−log axes against degree of polymerization of the diffusing chain, N. Data refer to diffusion in solution (circles) and to surface diffusion (squares). A schematic diagram of a two-dimensional pancake is included. Lines with slopes $-1/2$ and $-3/2$ are drawn for comparison. Temperature was 22 °C. Uncertainty of the measurement, ±20%, is of the size of the symbols. The dashed lines represent the best fit of the data points to a power law with powers −0.48 and −1.49, respectively.

against the delay time, τ. The lines drawn through the data show the fits to a single species model with diffusion restricted to a two-dimensional experimental geometry.[27] The agreement between data and fit confirms a single diffusion time. The fit to the autocorrelation function determined the mutual diffusion coefficient (D_M), but as noted above in the Experimental Section, in dilute systems such as the present experiment $D_M \approx D_{CM}$ (D_{CM} is the center-of-mass diffusion coefficient).

In the data shown in Figure 4, the measured diffusion coefficient, in the bulk and on the surface, is plotted, on a log−log scale, against the degree of polymerization of the adsorbed PEG chains. The data for surface diffusion show $D \sim N^{-3/2}$ (see Discussion section). Data for diffusion in the bulk solution are consistent with the hydrodynamic result, $D \sim N^{-1/2}$, known from prior measurements on the PEG system.[28] This is the standard result for an ideal chain in dilute three-dimensional solution with full hydrodynamic interaction. Note that these data concerning bulk diffusion suggests that conformation of PEG of these chain lengths in aqueous solution under these conditions constituted a random coil (though helical conformation has been suggested theoretically[29] and experimentally[30]). This is consistent with data reported earlier by many other groups.[28,31]

Water is a good solvent at 25 °C for PEG, but for short chains in good solvent conditions in the bulk, $D \sim N^{-1/2}$ is observed phenomenologically because asymptotic scaling laws characteristic of excluded volume in three dimensions are not yet reached.[32] In the asymptotic limit of very high molecular weight, the power law would be 0.6.

When considering these chains in the dilute surface-adsorbed state, excluded-volume statistics may apply for equilibrium properties. Excluded-volume chain statistics are enhanced by a situation of reduced dimensionality since coil density is larger. Moreover, the existence of discrete adsorption sites on OTE and surface topography may also perturb the polymer conformation in a manner difficult a priori to predict.

The diffusion data were reproducible within ±15% when the measurement was made repeatedly at different points on the same surface or repeated in independent setups (new OTE surface, new polymer labeling) on different months. This amount of uncertainty is the size of the symbols in Figure 4. As the surface coverage was never exactly the same in independent setups, the lack of dependence on surface coverage is consistent with our contention that the adsorbed chains were indeed in the dilute regime.

Discussion

The key puzzle is to understand the surface self-diffusion law, $D \sim N^{-3/2}$. This simple and clean fractional power is unlikely to reflect a coincidence or accident of experimental system chosen. It is worth emphasizing that this power law emerged persuasively when N was varied by more than an order of magnitude and that scatter of the data was low. Pending comparison with other systems (this being the first of which we are aware), we tentatively seek explanation in terms of general physical principles. However, many possible explanations seem plausible to us at this time. The diversity of dynamical transport scenarios is compounded by the fact that polymer diffusion is sensitive to chain conformation on the surface which is not directly observable. Hence, our modest goals are twofold. First, we analyze the equilibrium adsorption isotherm data for hints as to polymer conformation. Second, we systematically present various dynamical mechanisms including suggestions for future experiments to more critically distinguish among various ideas.

A. Binding Energy and Chain Conformation. We begin by analyzing the dilute isotherm data for $N = 48$ given in the inset of Figure 2. Our goal is to estimate the polymer binding (free) energy and to critically examine our hypothesis that polymers exist as flattened pancakes which have an N-independent thickness normal to the surface and a swollen self-avoiding walk conformation parallel to the surface.

The classic Flory-like theory of de Gennes[33] for adsorption from dilute solution of a single, long ($N \gg 1$) self-avoiding-walk (SAW) chain is based on assuming

the chains are very strongly adsorbed, and the field-theoretic justified concept[34] of a renormalized attractive free energy per segment (in units of kT) is defined as $-\delta$. There is a well-defined threshold (in temperature, T_c, or segmental attractive energy, ϵ_c) below which no adsorption occurs. The dimensionless parameter δ is measured relative to this threshold and can be expressed as either $(T_c/T) - 1$ or $\epsilon/\epsilon_c - 1$. If $\delta < 0$, no adsorption occurs. Neglecting numerical prefactors, and taking into account excluded-volume effects in the layer (so-called "proximal" exponent correction[35]), yields the chain free energy relative to the bulk state as a function of layer thickness, H:

$$\beta F(H) = N(\sigma/H)^{5/3} - N\delta(\sigma/H)^{2/3} \tag{2}$$

where σ is the statistical segment length and $\beta = 1/kT$. Minimization of eq 2 yields the equilibrium layer thickness and adsorption free energy

$$H = 5\sigma/2\delta, \quad \beta E_A \equiv -N\delta^{5/3}/3 \tag{3}$$

de Gennes has also derived a simple expressed for the adsorption isotherm under dilute coverage conditions:[33]

$$\Theta \approx \rho a^3 \exp(-\beta E_A) \tag{4a}$$

where Θ is the fractional coverage, ρ the monomer number density, and "a" the monomer diameter. Under melt conditions, $\rho_{melt}a^3 \approx 1$, allowing eq 4 to be rewritten in terms of a reduced polymer concentration:

$$\Theta = (\rho/\rho_{melt}) \exp(-\beta E_A) \tag{4b}$$

From the inset of Figure 2, one finds for the $N = 48$ PEG sample that $\theta \approx 0.05$ when $\rho/\rho_{melt} \approx 0.0002/1.2$, where we have used the known melt density of PEG. Employing these experimental numbers in eq 4b yields a polymer chain total binding energy of $E_A \approx -5.7kT$. Application of eq 3 then yields $\delta \approx 0.54$ and $\delta N^{3/5} \approx 5.5$. The latter quantity is a dimensionless measure of the propensity to adsorb and form a flattened pancake conformation. Physically, it represents the net adsorption energy if a 3-dimensional SAW polymer contacts a flat surface. Pancake conformational behavior emerges when this parameter is sufficiently large (see below). The de Gennes analysis implicitly assumes long chains and thus $\delta N^{3/5} \gg 1$.

The question arises as to the quantitative applicability of the large N de Gennes analysis (with prefactors ignored) to the rather modest degree of polymerization systems of our experiments. Fortunately, Monte Carlo simulations have recently studied this problem quantitatively for chain lengths of $N = 30-100$. In particular, Lai[36] employed the fluctuating bond model to study adsorption of a single SAW chain (monomer diameter, d) onto a flat smooth wall. The attractive wall-segment adsorption energy at contact is defined as $-\epsilon$, and the adsorption transition was deduced to occur at a temperature $T_A \approx 0.92\epsilon$. For $T < T_A$, the adsorption energy was found to be

$$E_A/\epsilon N^{3/5} \sim -(4/3)(\delta N^{3/5})^{2/3} \tag{5}$$

where $\delta = 1 - (T/T_A) = 1 - (1.09/\beta\epsilon)$. Equation 5 can be rewritten as

$$\beta E_A/N = -(4/3)\beta\epsilon[1 - (1.09/\beta\epsilon)]^{2/3} \tag{6}$$

Employing the $N = 48$ dilute adsorption data of Figure 2 and eq 6 yields $\delta = 0.37$ and $\delta N^{3/5} = 3.8$. These values are close to those obtained using eq 4, and their smaller magnitude is perhaps expected based on finite N crossover corrections relevant for our experimental systems. The fundamental question is whether such values are consistent with the $N = 48$ polymer being in a pancake conformation.

Examination of the results of Lai[36] clearly show the answer to be affirmative, as we briefly summarize. For a value of $\delta = 0.37$, or equivalently a reduced temperature of $T/T_c = 0.63$, the simulations find a layer thickness $H < 2d$, which is nearly the asymptotic large N value, and for which the classic scaling law of $H \sim 1/\delta$ holds to a very good approximation. In addition, for $\delta N^{3/5} = 3.8$ the adsorption energy very nearly follows the asymptotic scaling behavior, the lateral chain dimensions obey the 2-dimensional SAW law, $R_{||} \sim N^{3/4}$, and the fraction of adsorbed segments is ≈75%.

Hence, by all metrics our $N = 48$ PEG chain appears to be well described by a pancake conformation. Such a conformation is further stabilized with increasing degree of polymerization,[33,34] and logic suggests that all adsorbed PEG chains are pancakes. Such a conclusion seems consistent with the strong, irreversible adsorption behavior discussed in the Experimental Section. However, the weak N dependence of the dilute isotherms in Figure 2 would appear to conflict with this interpretation since an exponential increase of the fractional coverage with N is expected. This point remains a puzzle and further experimentation is required including addressing the possible role of the dye on polymer conformation.

New experiments to carefully determine the adsorption isotherms using FTIR and unlabeled PEG chains are planned. Since the dye is relatively bulky, is a zwitterion, and does not adsorb onto the OTE surface, the question of conformational perturbation of PEG via long-range effective repulsive forces between the dye and the polarizable surface[37] deserves careful consideration. Since the dye is attached at only one end, its consequences are expected to be N-dependent. For example, it could frustrate attachment of PEG segments located near it. Such a complication would also depend on surface chemistry and dye molecular structure. For the purposes of this first study, we shall proceed under the assumption that the dye does not play a critical role and that the likely adsorbed polymer conformation is a classic pancake.

B. Transport Mechanisms. We now turn to a discussion of possible diffusion mechanisms. On the basis of the above parameters for the $N = 48$ sample, we note that perpendicular localization and a simple Rouse diffusion law, $D_{||} \sim N^{-1}$, are expected from the simulations.[36] In the classical Rouse model, the lateral forces exerted on the polymer are uncorrelated in space and time, yielding the simple result that the total friction on the chain center-of-mass scales with N.[10,12,38]

This behavior conflicts with our observations, which suggests that the dominant physics for transport in our experimental system is not contained in the simulation model. Possible omissions include solvent-mediated hydrodynamic interactions, nonathermal solvent qual-

ity, dynamical consequences of dye labeling on polymer transport (and conformation), and a nonflat surface with discrete binding sites and local free energy barriers.

Our intention in maintaining submonolayer surface coverage, <1% of the saturated value, was to study the lateral diffusion of isolated chains. We first critically examine our contention of dilute coverage ($c_{2D} \ll c^*_{2D}$, the dilute−semidilute crossover in two dimensions) in order to rule out polymer−polymer interactions as a possible complication.

For the sake of argument, we adopt the standard idea[13,34] that in good solvents the (quasi) 2-D adsorbed random coil obeys self-avoiding walk statistics, $R_{||} \sim N^{3/4}$. The persistence length of PEG in bulk aqueous solution is ≈3 Å.[39] The average number of molecules within the excitation area of the laser beam was estimated from the fluctuation amplitude $g(0)$ to be 50 for the chains with $N = 48$, 113, and 456; it was 20 for $N = 244$ and 25 for $N = 693$. Using these numbers, the surface concentration c_{2D} was calculated from the ratio of total area occupied by the adsorbed polymers to the area illuminated by the laser spot. We concluded that the polymer coverage was not higher than the crossover concentration, c^*_{2D}.

However, in the control experiments with polymers with $N = 113$, $N = 244$, and $N = 693$, we found that diffusion coefficient did not depend (within our experimental error) on the amount of adsorbed polymer over a wide range of surface on surface coverage up to ∼40%. Diffusion at higher surface coverage was not studied because we found that at concentrations higher than ∼500−800 nM the PEG chains in solution were partly aggregated.

B.1. First-Principles Formalism. The observed non-Rouse $D \sim N^{-3/2}$ diffusion law implies some kind of correlated motion of the segments of a single adsorbed chain. One can conceive of two possible origins of such correlation: solvent-mediated hydrodynamic forces, $\vec{F}_H$, and/or direct (Newtonian) surface-mediated forces, $\vec{F}_s$. Nonequilibrium statistical mechanics provides a formally exact expression for the center-of-mass self-diffusion constant parallel to the surface, $D_{||}$, in terms of the total friction, $\xi_{||}$:[40]

$$D = kT/\xi_{||}$$

$$\xi_{||} = (\beta/2)\int_0^\infty \mathrm{d}t \sum_{i,j=1}^{N} \langle \vec{F}^{//}_i(0)^* \vec{F}^{//}_j(t)\rangle \qquad (7)$$

where $\vec{F}^{//}_j(t)$ is the total force exerted by the solvent and surface on monomer j of the polymer at time t in the direction parallel to the surface plane. The hydrodynamic and through-space surface forces could be dynamically coupled resulting in important cross terms in eq 7.

Note that if the surface itself were mobile, in the sense that the rate-limiting process were tied to surface relaxation/flow, then uncorrelated Rouse dynamics may be expected (assuming screening of hydrodynamic interactions between different polymer segments). This corresponds to vanishing of the nondiagonal terms in eq 7 and recovery of the $D \sim N^{-1}$ Rouse scaling law as observed for electrostatically adsorbed DNA on a fluid cationic lipid membrane.[13]

On a solid surface, however, adsorption sites are nearly static. Moreover, the fluid surface provides an effective dissipative bath for rapid momentum transport and hence screening of hydrodynamic interactions, a process not necessarily operative at a solid interface. Note also that the observation of Rouse dynamics in the simulations[36] is consistent with expectations based on eq 7 since the model neglects hydrodynamic interactions and employs a smooth wall, in which case the lateral polymer−surface forces vanish.

In general, first-principles evaluation of the friction term in eq 7 is impossible. Recently, modern statistical dynamical methods have allowed significant progress to be made for describing slow entangled dynamics in dense polymer solutions and melts.[40] Nonlocal friction effects and correlated segmental motions are captured, and microscopic connections between structure and transport are identified.

However, generalization of such a first-principles approach to treat the highly anisotropic problem of a single chain strongly adsorbed to a structured surface remains a formidable challenge. Knowledge of the energy landscape that the adsorbed polymer experiences, of the static density fluctuations and long-time collective dynamics (phonons) of the surface groups, and of hydrodynamic coupling are all, in principle, required. Thus, strong physical idealizations and/or bold Ansatzes appear necessary for progress at this time, and this is our present focus. In the discussion that follows, we consider separately, at a crude qualitative level, the possible consequences of hydrodynamic and polymer−surface frictional processes.

We first ignore hydrodynamic interactions except at the single segment level where they serve to determine the elementary time scale, or local friction constant, via the standard Stokes−Einstein treatment.[38] The polymer is assumed to remain attached to the surface so that the parallel diffusion constant is controlled exclusively, or primarily, by lateral dynamical motions.

B.2. The Reptation Scenario. A polymer pancake on the OTE surface experiences a rough energy landscape of local minima (binding sites) and maxima separated by distances of order a methyl group diameter. If these barriers are assumed to be large, polymer diffusion would proceed by correlated movement in the potential minima.

The possibility of some slack between sticking points, and hence of short loops that would constitute defects in the pancake structure, is an intriguing possibility (although seemingly impossible at this time to test by direct experiment at the dilute surface coverage of these experiments). Such a scenario would be akin to diffusion on a flat surface in the presence of impenetrable barriers or obstacles separated by some characteristic distance—a classical model of polymer transport in a gel.

Whether these obstacles would constitute defects in the monolayers on which the chains rest, or perhaps the corrugation between individual terminal methyl groups of the self-assembled monolayer on which it is adsorbed, or something else, is not known. Regardless, if there were some slack between sticking points, then one can imagine that loops of an isolated flexible chain might propagate efficiently along its length in a caterpillar-like fashion with adsorption sites playing a role analogous to entanglements in bulk systems.[38]

The scenario presented above suggests that a curvilinear, anisotropic reptative motion in a static "tube" might be relevant.[38] In the 2-D limit, the terminal relaxation time is still assumed to scale with the classic degree of polymerization cubed law, $\tau_D \sim \xi N^3$, indepen-

dent of solvent quality. Here, ξ is the local average segment friction constant which reflects both polymer−solvent and polymer−surface interactions. The real-space diffusion constant then follows from Fick's law:

$$D \sim R_g^2/\tau_D \sim N^{-3+2\nu} \tag{8}$$

where $R_g \sim N^{\nu}$. Equation 8 has been verified via simulation assuming reptation-like dynamics for self-avoiding chains.[41]

For polymer coils adsorbed on a rough adsorbing surface, whether the chain statistics are SAW or ideal is not obvious. Thus, this reptation mechanism can result in the following diffusion laws:

$$D \sim N^{-3/2}, \quad \text{2-D SAW}$$
$$D \sim N^{-2}, \quad \text{ideal} \tag{9}$$

The prediction for good solvent scaling agrees with our experiment. For this mechanism to hold down to relatively short chains of $N = 48$ would require rather tightly spaced obstacles.

However, we emphasize many caveats. Even if the analogy to diffusion in a 2-D gellike obstacle net is realistic, the diffusion scaling law is generally nonuniversal as emphasized by Muthukumar,[42] Zimm,[43] and others. For example, for experimentally relevant degrees of polymerization, details such as the spacing of obstacles, polymer−obstacle enthalpic interactions, and whether the obstacles are regularly or randomly distributed in space, can all influence apparent scaling exponents. Slater and Wu[12] find that the magnitude of the scaling exponent can vary over the range of −1 to −2.3 depending on the (randomly placed) obstacle concentration. On the other hand, for regularly placed obstacles, recent simulations find a clear $D \sim N^{-3/2}$ law for the case of a single value of widely separated obstacles.[11] Further simulations regarding this question are desirable.

B.3. The Amoeba Scenario. An alternative idea suggested by de Gennes[44] assumes that the polymer pancake obeys ideal statistics, in which case it is a dense (space-filling) fluctuating disk. Inside the disk, the high density results in high friction and binding sites are nearly saturated. Thus, it is hypothesized that the rate-limiting process for diffusion is random hopping of the segments along the circumference of the fluctuating disk which can more easily jump into empty binding sites with a lower friction, thereby allowing the interior segments to subsequently locally hop. The physical picture is of a highly correlated, isotropic "amoeba-type" motion with transport controlled by local barrier hopping between binding sites of the disk perimeter monomers.

In terms of the displacement of segments j, $\Delta\vec{r}_j(t)$, the center-of-mass mean-square displacement is given by

$$\langle \Delta\vec{R}_{CM}^{\,2}(t)\rangle = N^{-2}\sum_{ij}\langle \Delta\vec{r}_i(0)\,\Delta\vec{r}_j(t)\rangle$$
$$\sim N^{-2}\sum_{j\epsilon_{\text{perimeter}}}\langle \Delta\vec{r}_j(0)\,\Delta\vec{r}_j(t)\rangle$$
$$\sim (d^2/\tau_{\text{jump}})(t/N^2)N^{1/2} \tag{10}$$

where d^2/τ_{jump} is the elementary jump diffusion constant, and the factor of $N^{1/2}$ is proportional to the number of perimeter sites of a 2-dimensional ideal random walk. Equation 10 plus Fick's law then yields

$$D \sim N^{-3/2}, \quad \tau_D \sim R_g^2/D \sim N^{5/2} \tag{11}$$

Thus, the observed N-scaling of the self-diffusion constant is again obtained for this very different ansatz for the motion mechanism, but it differs from the ideal-coil reptation idea above and the N-scaling of the terminal relaxation time is also different.

B.4. The Sticky Reptation Scenario. A third variation follows from assuming a loop−train−tail polymer conformation[25] fundamentally distinct from a pancake conformation. Diffusion would proceed by the transient liftoff of loops followed by readsorption at a new random position.

Such a situation would seem to be appropriate only by accident at dilute polymer coverage if the system were very close to the adsorption threshold, which does not seem consistent with our adsorption isotherm measurements. Moreover, being close to threshold is seemingly impossible to achieve for the wide range of degrees of polymerization studied in these experiments, and the combination of strongly loopike conformations and strong adhesive pinning sites on the surface seems physically unrealistic. Nonetheless, it is interesting and instructive to examine the dynamical consequences of this model in order to further emphasize the many different scenarios by which the observed N-scaling can be rationalized.

For this situation, the number of adsorption contacts between the polymer and surface scales as N^{ν}, where ν is the bulk 3-D dilute solution R_g scaling exponent. If one assumes that such contacts are "pinned", then transport would occur only via stochastic sliding of the chain through the contact points. Such a "sticky reptation" mechanism corresponds to a tube diffusion constant given by[45]

$$D_{\text{TUBE}} \sim kT/(N\xi_0 + bN^{\nu}\xi_s) \tag{12}$$

where ξ_0 is the segment friction coefficient due to collisions with the solvent, and ξ_s is the analogous quantity due to segment−surface adhesive contacts (b is a number of order unity). If the attractions are strong, which is consistent with the assumption that they represent pinning points, then $\xi_0 \ll \xi_s$. Thus, for modest degrees of polymerization one may have $N\xi_0 \ll bN^{\nu}\xi_s$. Under this situation, the chain terminal relaxation time scales as

$$\tau_D \sim N^2/D_{\text{TUBE}} \sim \xi_s N^{2+\nu} \tag{13}$$

Combining eqs 12 and 13 with Fick's law yields the laboratory 2-D self-diffusion constant:

$$D \sim R_g^2/\tau_D \sim N^{-2+\nu}$$
$$\sim N^{-3/2}, \quad \text{ideal}$$
$$\sim N^{-7/5}, \quad \text{SAW} \tag{14}$$

In this scenario, there is little difference between ideal and good solvent conditions, and again agreement with the observed scaling can be obtained (exactly or approximately), although based on a model of very questionable applicability. Note that the chain relaxation time scaling for ideal conditions also coincides with that

from the "amoeba" model above, but not with the 2-D reptation model.

B.5. The Hovercraft Scenario. Our understanding of the consequences of solvent-mediated hydrodynamic forces on macromolecular transport near surfaces is relatively primitive. However, one can envision dramatic effects if the polymer exists as a pancake on (or close to) the surface and moves cooperatively with the solvent molecules which inhabit its macromolecular domain. In this case the cross-sectional area of the 2-D SAW chain scales as $N^{3/2}$. Hence, if one postulates that the friction between the polymer−solvent complex with the surface scales with contact area,[46] one again obtains the $D \sim N^{-3/2}$ law. Such an idea is quite general with regards to polymer shape, and an argument for the total friction constant such as just presented applies if there is a thin (N-independent) layer of solvent separating the macromolecule and the surface.[46]

Conclusion and Prospects

Many of the very different scenarios for transport presented above are consistent with our observation that $D \sim N^{-3/2}$. How to distinguish among them is difficult, although measurement of the chain relaxation time would provide some discriminatory information. Clearly, much more extensive experimentation is needed to make further progress. Systematic variation of the polymer−surface interaction, surface topography (e.g., patchy adsorbing surfaces), and solvent quality would be valuable to probe the robustness of the present diffusion law. These variables would perhaps serve to modify the polymer conformation and discover its dynamical consequences. Increasing the surface coverage such that polymer−polymer interactions come into play would also be interesting, although major changes in polymer conformation and layer thickness are expected to occur. Finally, a more advanced theoretical treatment of the many aspects sketched above it needed. Benchmark computer simulations for a single adsorbed chain on a corrugated surface with, and without, hydrodynamic interactions would also be very valuable. With the rapidly expanding technological developments in computer power, simulations of such a problem with explicit solvent may soon be feasible.

In summary, a strikingly strong power-law scaling of the surface diffusion coefficient with degree of polymerization has been observed for the lateral transport of a flexible polymer chain on a solid surface. A variety of speculative explanations have been identified and their elementary consequences explored. These serve to suggest new experimental and computation directions to follow in the quest for a definitive understanding of this fascinating problem.

Acknowledgment. For discussions, we are indebted to J. F. Douglas, P.-G. de Gennes, and M. Rubinstein. Support for this work was provided by the U.S. National Institutes of Health, Grant PHS 5 P41 RR03155 (Y.C., J.M., and E.G.) and the U.S. Department of Energy, Division of Materials Science, under Award DEFG02-91ER-45439, through the Frederick Seitz Materials Research Laboratory at the University of Illinois at Urbana−Champaign (S.A.S., K.S.S. and S.G.).

References and Notes

(1) Mansfield, K. F.; Theodorou, D. N. *Macromolecules* **1991**, *24*, 6283.
(2) Binder, K.; Milchev, A.; Baschnagel, J. *Annu. Rev. Mater. Sci.* **1996**, *26*, 107.
(3) Frank, B.; Gast, A. P.; Russell, T. P.; Brown, H. R.; Hawker, C. *Macromolecules* **1996**, *29*, 6531.
(4) Zheng, X. M.; Rafailovich, M. H.; Sokolov, J.; Strzhemechny, Y.; Schwarz, S. A.; Sauer, B. B.; Rubinstein, M. *Phys. Rev. Lett.* **1997**, *79*, 241.
(5) Forrest, J. A.; Dalnoki-Veress, K. *Adv. Colloid Interface Sci.* **2001**, *94*, 167.
(6) Rubinstein, J. L. R.; Smith, B. A.; McConnell, H. M. *Proc. Natl. Acad. Sci. U.S.A.* **1979**, *76*, 15.
(7) Peters, R.; Peters, K. *Proc. Natl. Acad. Sci. U.S.A.* **1983**, *80*, 7187.
(8) Almeida, P. F. F.; Vaz, W. L. C.; Thompson, T. E. *Biochemistry* **1992**, *31*, 6739.
(9) Kim, S. H.; Yu, H. *J. Phys. Chem.* **1992**, *96*, 4034.
(10) Carmesin, I.; Kremer, K. *J. Phys. (Paris)* **1990**, *51*, 915.
(11) Azuma, R.; Takayama, H. *J. Chem. Phys.* **1999**, *111*, 8666.
(12) Slater, G. W.; Wu. S. Y. *Phys. Rev. Lett.* **1995**, *75*, 164.
(13) Maier, B.; Rädler, J. O. *Phys. Rev. Lett.* **1999**, *82*, 1911. Maier, B.; Rädler, J. O. *Macromolecules* **2000**, *33*, 7185.
(14) Magde, D.; Elson, E. L.; Webb, W. W. *Biopolymers* **1974**, *13*, 29.
(15) Berland, K. M.; So, P. T. C.; Gratton, E. *Biophys. J.* **1995**, *68*, 694.
(16) Sukhishvili, S. A.; Chen, Y.; Müller, J. D.; Gratton, E.; Schweizer, K. S.; Granick, S. *Nature (London)* **2000**, *406*, 146.
(17) Rinderknecht, H. *Nature (London)* **1962**, *193*, 168.
(18) Der-Balian, G. P.; Kameda, N.; Rowley, G. L. *Anal. Chem.* **1988**, *173*, 59.
(19) Cohen Stuart, M. A.; Tamai, H. *Langmuir* **1988**, *4*, 1184.
(20) Kessel, C. R.; Granick, S. *Langmuir* **1991**, *7*, 532.
(21) Léger, L.; Hervet, H.; Rondelez, F. *Macromolecules* **1981**, *14*, 1732.
(22) So, P. T. C.; French, T.; Yu, W. M.; Berland, K. M.; Dong, C. Y.; Gratton, E. *Bioimaging* **1995**, *3*, 1.
(23) Frantz, P.; Granick, S. *Macromolecules* **1995**, *28*, 6915.
(24) Frantz, P. Granick, S. *Langmuir* **1992**, *8*, 1176.
(25) Fleer, G. J.; Cohen Stuart, M. A.; Scheutjens, J. M. H. M.; Cosgrove, T.; Vincent, B. *Polymers at Interfaces*; Chapman & Hall: London, 1993.
(26) Kuzmenka, D. J.; Granick, S. *Macromolecules* **1988**, *21*, 779.
(27) Thompson, N. L. Fluorescence Correlation Spectroscopy. In Lakowicz, J. R., Ed.; *Topics in Fluorescence Spectroscopy 1*; Plenum Press: New York, 1991.
(28) Yuko, K.; Chikako, H. *Polym. Commun.* **1984**, *25*, 154.
(29) Tasaki, K. *J. Am. Chem. Soc.* **1996**, *118*, 8459.
(30) Matsuura, H.; Fukuhara, K. *J. Mol. Struct.* **1985**, *126*, 251.
(31) Waggoner, R. A.; Blum, F. D.; Lang, J. C. *Macromolecules* **1995**, *28*, 2658.
(32) Huber, K.; Bantle, S.; Lutz, P.; Burchard, W. *Macromolecules* **1985**, *18*, 1461.
(33) de Gennes, P.-G. *J. Phys. (Paris)* **1976**, *37*, 1445.
(34) Eisenriegler, E. *J. Chem. Phys.* **1983**, *79*, 1052. Eisenriegler, E.; Hanke, A.; Dietrich, S. *Phys. Rev. E* **1996**, *54*, 1134.
(35) de Gennes, P.-G. *J. Phys., Lett.* **1983**, *44*, 241.
(36) Lai, P.-Y. *Phys. Rev. E* **1994**, *49*, 5420.
(37) Israelachvili, J. N. *Intermolecular and Surface Forces*, 2nd ed.; Wiley: New York, 1992.
(38) Doi, M.; Edwards, S. F. *Theory of Polymer Dynamics*; Clarendon Press: Oxford, 1986.
(39) Faraone, A.; Magazù, S.; Maisano, G.; Migliardo, P.; Tettamanti, E.; Villari, V. *J. Chem. Phys.* **1999**, *110*, 1801.
(40) Schweizer, K. S.; Fuchs, M.; Szamel, G.; Guenza, M.; Tang, H. *Macromol. Theory Simul.* **1997**, *6*, 1037.
(41) Leegwater, J. A. *Phys. Rev. E* **1995**, *52*, 2801.
(42) Muthukumar, M.; Baumgartner, A. *Macromolecules* **1989**, *22*, 1937.
(43) Zimm, B. H.; Lumpkin, O. *Macromolecules* **1993**, *26*, 226.
(44) de Gennes, P.-G., private communication.
(45) Zheng, X.; Sauer, B. B.; Van Alsten, J. G.; Schwarz, S. A.; Rafailovich, M. H.; Sokolov, J.; Rubinstein, M. *Phys. Rev. Lett.* **1995**, *74*, 407.
(46) Hubbard, J. B.; Douglas, J. F. *Phys. Rev. E* **1993**, *47*, R2983.

MA0113529